Simulation and analysis on the property of aluminum back-surface-field of monocrystalline silicon solar cells

X. L. CAO, Y. M. CHEN*
School of Energy Science and Engineering, Central South University, Changsha410083, P. R. China

The effects of thickness and doping profile of heavily-doped Aluminum Back-Surface-Field(Al-BSF), as well as the trap levels of impurities in Al-BSF, on electronic properties of n^+pp^+ monocrystalline solar cells, were investigated by PC1D. The results show the electronic properties of the solar cells are hardly affected by the gradient of the doping profile of Al-BSF, but mainly depend on the Al/B atomic amount in Al-BSF. The optimum thickness of Al/B-BSF is about 10μm with the average Al/B atomic concentration of Al-BSF less than ~$6.56\times10^{18}cm^{-3}$. The effect of the oxygen trap level on the electronic properties relates to the back surface recombination velocity (BSRV) and the average Al/B atomic concentration.

(Received December 20, 2010; accepted April 11, 2011)

Keywords: Al-BSF, Electronic property, Doping profile, The trap level

1 Introduction

The Al-BSF can improve greatly electronic properties of solar cells, and therefore it is widely used in all kinds of high efficiency solar cells [1-3]. In addition, the Al-BSF more and more attracts photovoltaic specialists' attention because of its high output rate, as well as its low cost. To prepare an Al-BSF in the processing industries, there are three main steps: (1) printing the aluminum paste on the back surface of silicon solar cells by Screen Printer, (2) sintering above the eutectic temperature, (3) regrowing epitaxially into a p+ layer containing Al or B in accordance with Al-Si phase diagram during cool-down[4-5]. Thereby a high-low pp+ junction was formed and its built-in electric field can effectively prevent photogenerated minority carriers from recombining at back surface of solar cells.

At present, the study on the Al-BSF concentrates mainly on its forming processes and the effect of Al-induced gettering[6-7]. This is due to close relationship between forming process of back-surface-fields and its functions. Aluminum atomic concentration of the Al-BSF is mainly determined by peak sintering temperature, and its doping profile is greatly influenced by Al-Si phase diagram during cool-down and the solid solubility of Al in silicon, and the thickness of the Al-BSF is chiefly determined by the initial thickness of aluminum paste on silicon substrate[8]. Generally, the functions of the Al-BSF enhance with its thickness and aluminum atomic concentration. Especially, the back surface passivation is related with thickness and aluminum-doped atomic concentration of the Al-BSF[9-11]. Therefore, a higher sintering temperature and a thicker thickness are necessary to prepare an Al-BSF with outstanding performance.

With the gradual decrease of substrate thickness of solar cells, a higher temperature and a thicker aluminum film both cause a great bowing of solar cells[12], which leads to a great increase of cost of solar cells. Photovoltaic specialists have found that the Al paste with boron-doped was helpful to increase the impurity concentration of Al-BSF, whose active peak Al/B atomic concentration could reach around $3\times10^{19}cm^{-3}$[13-14]. In this page, with the purpose of providing theory for optimizing the preparation processes of the Al-BSF, the effects of thickness, the average Al/B atomic concentration and the gradient of the doping profile, as well as the trap level of impurities in Al-BSF, on electrical properties of n^+pp^+ monocrystalline solar cells, were investigated by PC1D.

2. The structure of solar cells and simulation details

The structure of the crystalline silicon solar cells used in this paper is n^+pp^+, as shown in Fig.1. The p-type base presented 1.6 Ω·cm, corresponding to background doping density of $9.137\times10^{15}cm^{-3}$, and its thickness is 180μm. In order to put the Al-BSF characteristics into evidence, the Gaussian n^+ emitters has a peak density of $3.982\times10^{19}cm^{-3}$ at the front surface, which is rather lower than that of the industrial solar cells, with the sheet resistance of ~100Ω/□ and the emitter junction depth of 0.5μm. What's more, the electron and hole lifetime parameters were set at 20μs and 90μs[15], respectively, corresponding to a excess-carrier lifetime of ~8.5ms in low-level injection and the corresponding diffusion length of ~5mm, for the excess carriers in material with the background doping density of $9.137\times10^{15}cm^{-3}$ at the temperature of 300K, which is far longer than the whole thickness of solar cells used in the simulation. The front surface recombination velocities S_f under the passivated regions dependent on the surface doping level, $S_p = 10^{-16}\times N_s$ cm/s($N_s>10^{18}cm^{-3}$) [16], was fixed at 4000cm/s, and the back surface recombination for the metal-contact regions are about $S_b = 1\times10^6$ cm/s.

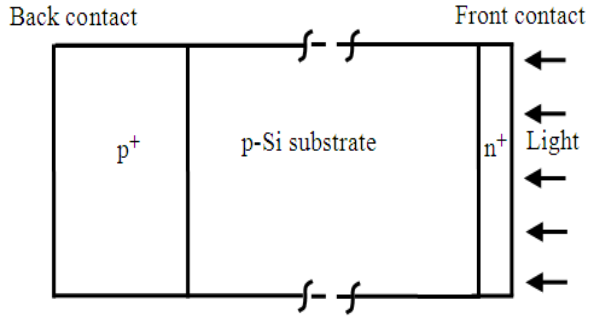

Fig.1 Schematic view of the monocrystalline silicon solar cell

The standard "terrestrial sun"-AM 1.5G was chosen as the illumination source, corresponding to an intensity of 0.1W/cm^2 at 25°C. In addition, the texture depths of the front and rear surface were both 0.2μm, and the front reflectance was fixed at 10% and the internal rear reflectance fixed into Lambert dispersion. Some essential parameters of monocrystalline silicon solar cells adopted in the simulations were shown in Table 1, and all of the other parameters were the default values in PC1D. The mobility models of holes and electrons as a function of local doping density at the temperature of 300K were also shown in Table 1.

Table 1 Some parameters values and models adopted in the simulations.

Parameters	n^+-Si layer	p-Si layer	p^+-Si layer
Dielectric constant	11.9	11.9	11.9
Bandgap (eV)	1.124	1.124	1.124
Electron Affinity(eV)	4.05	4.05	4.05
Minority carrier lifetime(μs)	---	20	---
Layer Thickness (μm)	0.5	179.5	Variable
Doping profile	Gaussian	Uniform	Variable
The trap level(eV)	E_i+0.514	E_i-0.516	Variable
Hole mobility (cm^2/V·s)	$155+315/[1+(N_D/1\times10^{17})^{0.9}]$	$37.4+432.6/[1+(N_A/2.82\times10^{17})^{0.642}]$	
Electron mobility (cm^2/V·s)	$60+1357/[1+(N_D/9.64\times10^{16})^{0.664}]$	$160+1257/[1+(N_A/5.6\times10^{16})^{0.647}]$	

During simulations and analysis, the effect of heavily-doping on the properties of solar cells was mainly considered. For p type and n type silicon, the energy bandgap narrowing model in this paper has the following form [17], respectively

$$\left.\begin{aligned}\Delta E_c &= 1.4\times10^{-2}\ln\left(\frac{N_D}{1.4\times10^{17}}\right)\\ \Delta E_v &= 1.4\times10^{-2}\ln\left(\frac{N_A}{1.4\times10^{17}}\right)\end{aligned}\right\} \quad (1)$$

Besides, in either heavily doped or highly injected material, the Auger recombination dominates compared with other recombination mechanism. To properly compute the Auger recombination effect, three Auger recombination coefficients are necessary to require, because in high-level injection the excess electron and hole concentrations are similar, and so the n-type and p-type coefficients in high-level injection are included as a single factor C_{HLI}, and the n-type coefficient C_{nLLI} and the p-type coefficient C_{pLLI} apply to material in low-level injection. The high-injection coefficient represents the sum of both n-type and p-type Auger recombination. The recombination rate due to the Auger processes is calculated from the following expressions [18]

$$U_{Auger} = \left(C_n n + C_p p\right)\left(pn - n_{ie}^2\right) \quad (2)$$

$$C_n = C_{nLLI}\frac{N_D}{N_D + p} + \frac{C_{HLI}}{2}\frac{p}{N_D + p} \quad (3)$$

$$C_p = C_{pLLI}\frac{N_A}{N_A + n} + \frac{C_{HLI}}{2}\frac{n}{N_A + n} \quad (4)$$

where C_{nLLI}= 2.2e^{-31}cm^6/s, C_{pLLI}= 9.9e^{-32}cm^6/s, C_{HLI}= 1.66e^{-30}cm^6/s.

3 Results and discussion

3.1 The gradient of the BSF doping profile

According to Ref.[11,13,19], four solar cells were assumed and marked with A、B、C and D, respectively, where the Al-BSF doping profiles of the solar cells A、B and D were Gaussian, but that of the solar cells C was uniform. However, the gradient of the four Al-BSF doping profiles was different from each other, as illustrated in Fig. 2. The thickness of the four solar cells was the same as 10μm.

In accordance with the theory of back-surface-field, the improvement in open circuit voltage resulting from the back surface field can be represented by [20]

$$\Delta V_{oc} \approx \frac{kT}{q}\ln\left[\frac{D_n}{N_A L}\int_{L-W_{jb}}^{L}\frac{N_A^+}{D_n^+}dx\right] \quad (5)$$

where N_A and N^+_A represent the doping concentration of the bulk and BSF region, respectively. And L and W_{jb} denote the thickness of the solar cell and the BSF region respectively. D^+_n represents the electron diffusivity in the BSF region, which nearly becomes a constant which is independent of the doping profile when the BSF region is doped heavily, and D_n represents the electron diffusivity of the p-type region. It can be known from Fig.2 that the open circuit voltage of the four solar cells is equal, which

indicates the doping amount is close to each other according to Eq. 5. Besides, the conversion efficiency and the short-circuit current of the four solar cells, as well as the fill factor, are also almost close.

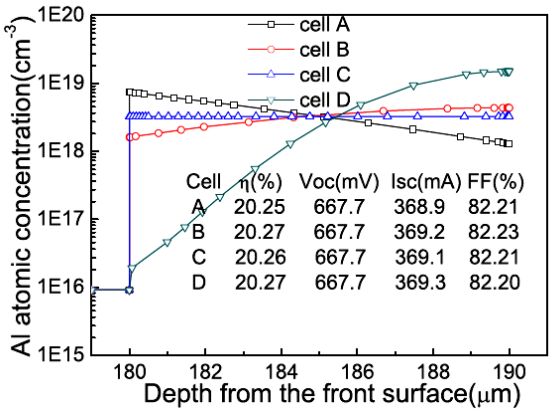

Fig.2 The effect of the gradient of the BSF doping profile on the electronic properties of solar cells

On the other hand, from the point of view of the energy bands of the pp^+ junction, as shown in Fig. 3, for the three cells with an abrupt rear junction BSF, it was found that the barrier height of the solar cell A is slightly higher than that of the other two cells, which means the Al-BSF of the cell A prevents more effectively the minority-carriers from recombining compared with the others. In particular, although the Al-BSF of the cell D can be approximately regarded as a linear graded junction, it also plays a great role in passivating the back surface, as well as the high-low junction at all, because the output parameters of the cell D are almost equivalent with the other three, and even a bit better. Besides, the effect of bandgap narrowing on the short circuit current of the solar cell A is the greatest, which is also consistent with Fig.2.

Further, in point of the effective back surface recombination velocity (S_{eff}), due to the different actual gradient of the doping profiles the solar cells may have different S_{eff}. However, according to the relationship between S_{eff} and doping concentration in the BSF region[5], S_{eff} is still difficult to calculate. Even so, the S_{eff} can still be reflected by the $J_{0,BSF}$, which is the saturation current density of the BSF at the back surface, in another way.

For a p^+p junction formed on a lowly injected p-type wafer with acceptor density N_A, the relation between S_{eff} and $J_{0,BSF}$ is[21]

$$S_{eff} = J_{0,BSF}\frac{N_A + \Delta n}{qn_i^2} \quad (6)$$

where Δn denotes the density of the excess electron carrier at the back surface. Besides, the $J_{0,BSF}$ is influenced by the gradient of the BSF doping profiles and for the above four cells it is between $8\times10^3$and 9×10^3 fA/cm^2 by calculating with PC1D, corresponding to S_{eff} of 4.7×10^4 ~5.1×10^4 cm/s by Eq. 6. Now, to interpret the effect of the gradient of the doping profile on the S_{eff} and the output performance of solar cells, the $J_{0,BSF}$ was assumed to vary from 1×10^1 to 1×10^5 fA/cm^2, which was realized by changing the trap level at the back surface. The electronic properties of the four solar cells as a function of $J_{0,BSF}$ are shown in Fig.4. As can be seen from Fig.4, the electronic properties of the solar cells rise with the decrease in the $J_{0,BSF}$. When the $J_{0,BSF}$ is less than ~10^3 fA/cm^2 the disparity of output parameters among the four cells is very small and even negligible. But the disparity is very difficult to distinguish with the $J_{0,BSF}$ is more than ~10^3 fA/cm^2. For industrial solar cells, the $J_{0,BSF}$ is of the order of magnitude of ~10^3 fA/cm^2 [22-23], and therefore the gradient of the BSF doping profiles have a smaller impact on the electronic performance of solar cells. Hence, we can conclude that the electronic properties of solar cells are completely independent of the gradient of the BSF doping profiles within the variations chosen here, which are rather small.

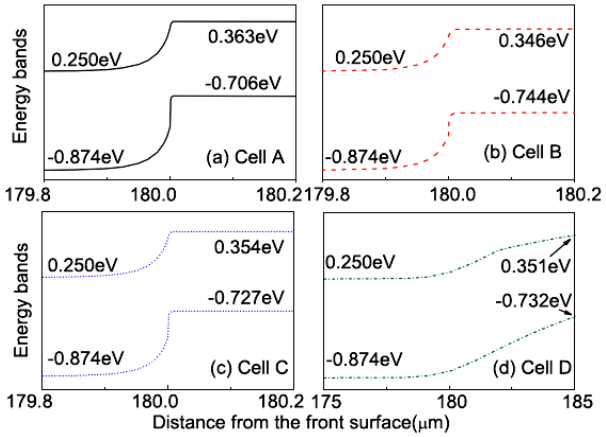

Fig.3 The bandgap diagram of pp^+ junction.

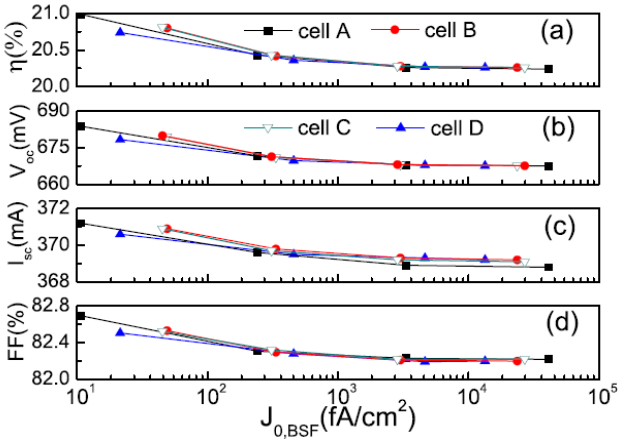

Fig.4 The electronic properties of solar cells as a function of $J_{0,BSF}$

3.2 The thickness of Al-BSF and the average Al/B atomic concentration

The aluminum atomic concentration in silicon is about 3×10^{18}cm^{-3} at the common sintering temperature of around 850°C. In this case, the electrical properties of solar cells generally improve with the increase of the

thickness of Al-BSF. However, the Al/B atomic concentration of the Al/B-BSF increased almost by an order of magnitude, because of aluminum paste with boron-doped. We supposed Al/B-BSF doping profile was Gaussian and its peak Al/B atomic concentration of $3\times10^{19}cm^{-3}$ were located at 2.5μm and 5.0μm from the back surface, respectively[13-14,19,]. Besides, Al/B-BSF thickness changed between 1μm and 30μm. In this conditions, the electrical properties of solar cells as a function of the Al-BSF thickness is illuminated in Fig.5.

As is shown from Fig.5, the electrical properties of cells initially increase with the thickness of Al/B-BSF, but when the Al/B-BSF thickness exceed some critical value, the conversion efficiency and the shout circuit current slowly descend, and the open circuit voltage keep a plateau. However, the fill factor increased at all times with increasing the BSF thickness mainly due to heavy doping reducing the series resistance of the solar cells. It may be accounted for this phenomenon that as the thickness of Al/B-BSF gradually increases the average Al/B atomic concentration of Al/B-BSF rises by degrees, and heavy doping leads to a more and more obvious negative effect on electrical properties of solar cells, and thus the electrical properties of the cells also decay by degrees. What's more, it is of note that the critical values are different for conversion efficiency and shout circuit current, which will be discovered later.

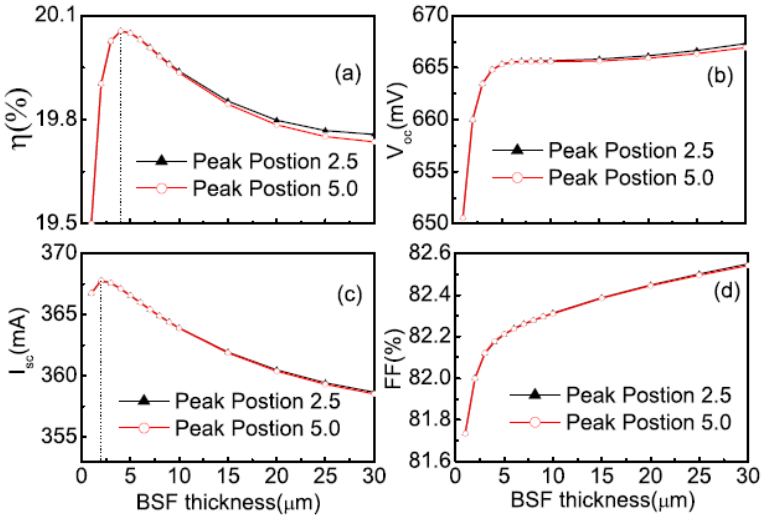

Fig.5 The electronic properties of solar cells as a function of thickness the Al/B-BSF with Gaussian doping profiles: (a) conversion efficiency (b) open circuit voltage (c) short circuit current (d) fill factor

In order to further obtain the critical average Al/B atomic concentration, we assume that Al/B-BSF doping profile is uniform, with Al/B atomic concentration in the range of $1.6\times 10^{18}cm^{-3}$ and $2\times10^{19}cm^{-3}$ and the thickness of the Al/B-BSF between 1μm and 30μm. As can be seen from Fig.6, when the average Al/B atomic concentration exceeds the value of about 6.56×10^{18} cm^{-3} and the Al-BSF thickness is more than 10μm, the electronic properties except the fill factor are beginning to slow down gradually. Besides, when the average Al/B atomic concentration is close to $2 \times 10^{19}cm^{-3}$, the photoelectric conversion efficiency and short-circuit current of solar cells are at all times in sharp decline with the thickness more than around 10μm, but the open circuit voltage has a gradual downward trend when the Al BSF thickness is more than 10μm. Obviously, this seems contrary to the Eq. 5, which indicates the Eq. 5 has been not applicable in this case of the average Al/B atomic concentration of Al/B-BSF close to $2\times10^{19}cm^{-3}$ owing to the bandgap narrowing effect and the Auger recombination[24]. The reason for the decrease of the short circuit current may be that the diffusion length of minority carriers in the region of Al/B BSF is further less than the BSF thickness so as to reduce the collection efficiency of minority carriers in the BSF region.

To account for this relation and the critical point mentioned above clearly, the output parameters as a function of the rate of the BSF thickness (W_{BSF}) to the diffusion length (L_{BSF}) of minority carries was discussed, as illuminated in Fig.7. From the Fig.7, it is obvious that the shout circuit current start to decline when the critical rate (W_{BSF}/ L_{BSF}) is about between 0.5~1, while for the conversion efficiency and open circuit voltage the critical rate is around between 1~2, which is always less than that of the shout circuit current because the open circuit is still on the increase when the short circuit current is on the decline with the BSF thickness. And this critical value can also be demonstrated in Fig.5, where the critical rates for I_{sc} and V_{oc} are about 0.8 and 1.6, respectively. However, in view of the conversion efficiency, the optimum thickness is about the diffusion length of minority carriers in heavily-doped BSF region.

To sum up, the electrical properties of solar cells enhance with the increase of the thickness of BSF when the average Al/B atomic concentration is less than 6.56×10^{18} cm^{-3}. The electronic properties of the solar cells are optimized if the average Al/B atomic concentration and thickness of Al/B-BSF are about $6.56\times10^{18}cm^{-3}$ and 10μm respectively. The optimum thickness of BSF declines sharply with the average Al/B atomic concentration of Al-BSF more than $1.15\times10^{19}cm^{-3}$ and mainly depends on the diffusion length of minority carriers in heavily-doped BSF region.

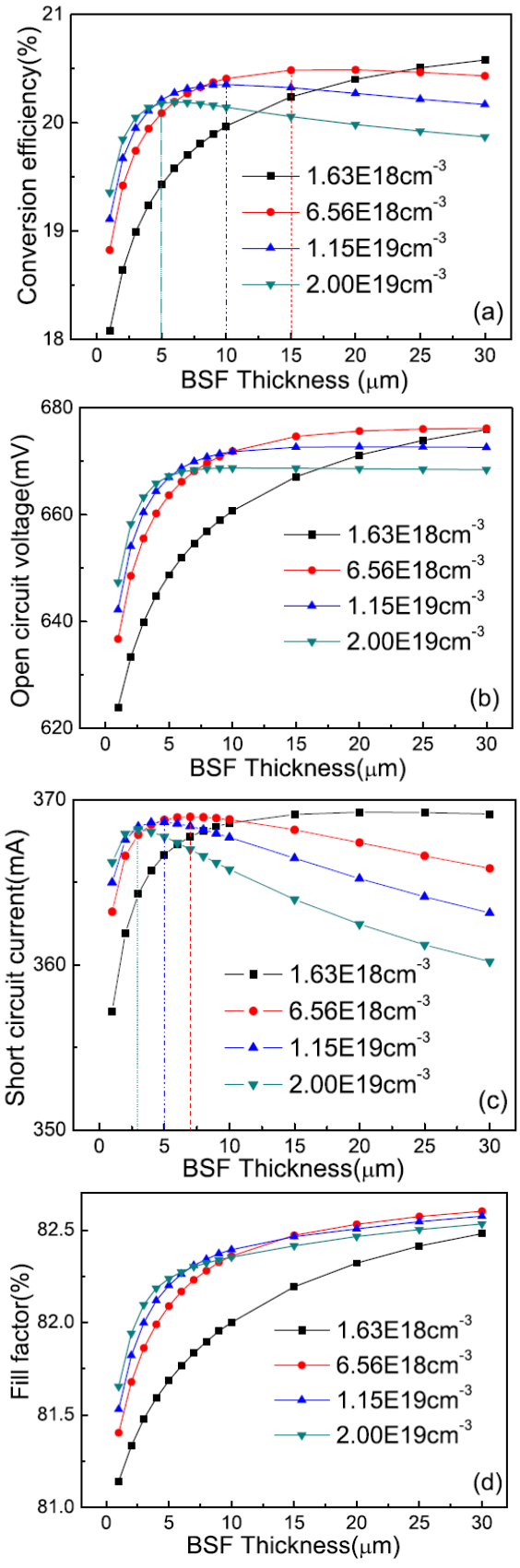

Fig.6 The electronic properties of solar cells calculated as a function of the thickness of Al/B-BSF with uniform doping profiles: (a) conversion efficiency (b) open circuit voltage (c) short circuit current (d) fill factor.

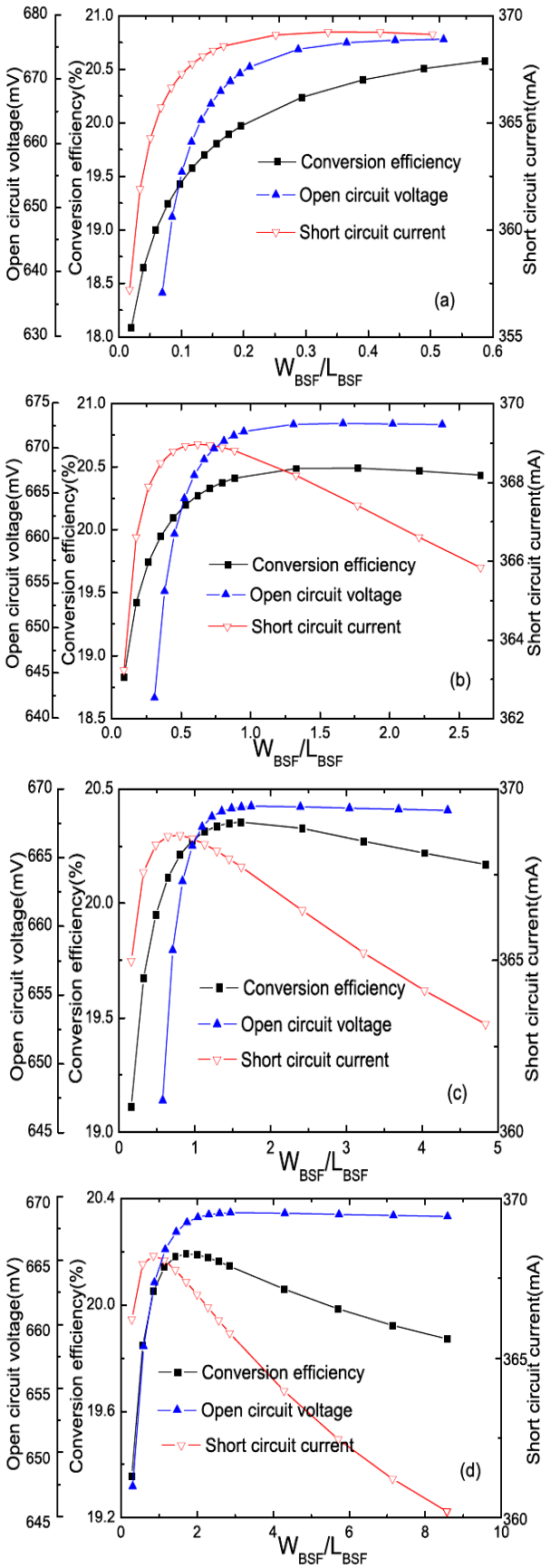

Fig7. The electronic properties as a function of the rate of the BSF thickness to the diffusion length of minority carriers in BSF region: (a) 51.1μm (b) 12.2μm (c) 6.2μm (d) 3.5μm.

3.3 The trap level of impurities in Al-BSF

The aluminum paste usually includes these impurities, such as C, O, Pb, Ni. But these impurities lead to some deep trap levels in silicon, which are just located near the center of silicon band gap and become most effective recombination centers [25]. Of course, the trap levels effect greatly not only the bulk recombination in region of Al/B-BSF, which can be reflected by the minority bulk lifetime, but also the back surface recombination. The deep trap level E_t is closely bound up with the Shockley-Read-Hall (SHR) surface recombination rate R_s, which is given in PC1D by the following expression[26]

$$R_s = \frac{S_n S_p \left(pn - n_{ie}^2 \right)}{S_p \left(p + n_{ie} e^{-E_t / kt} \right) + S_n \left(n + n_{ie} e^{E_t / kt} \right)} \qquad (7)$$

where S_n and S_p denote the electron and hole recombination velocity at the rear surface of solar cells, respectively. Besides, the aluminum and boron trap levels in silicon are E_i-0.507eV and E_i-0.518 eV, respectively. In our simulations, we assumed S_n and S_p were equal. In order to research the effects of the deep trap level on the electronic properties of solar cells, we take example for the oxygen impurity, because the oxygen trap level (E_i-0.152 eV) [25] is the nearest to the center of silicon band gap and therefore has a greater impact on the performances of solar cells compared with all above impurity trap levels.

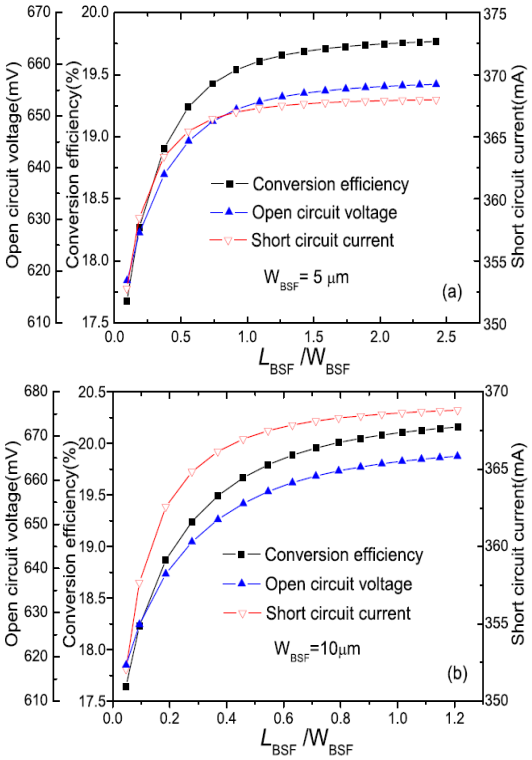

Fig.8 The effect of the SHR recombination in the BSF region on the electronic properties of solar cells: (a) with the BSF thickness of 5μm; (b) with the BSF thickness of 10 μm

Fig.8 illustrates the effect of SHR recombination via defects in the BSF region on the output performance of solar cells with the uniform Al/B atomic concentration in BSF region of 3.25×10^{18}cm^{-3}. As is shown in Fig.8, regardless of the BSF thickness, the output performance of solar cells increase at all times with lengthening the diffusion length of minority carriers in the BSF region. Especially, when the diffusion length of minority carriers in the BSF region is less than the BSF thickness, the solar cells output performance of sharply increase with the diffusion length of minority carriers increasing, which is obviously due to the collection efficiency of minority carriers in BSF region also illustrated in Fig.7.

Fig. 9 illustrates the effects of the oxygen trap level on the electronic properties of solar cells with the back surface recombination velocity between 1×10^{2}cm/s and 1×10^{7}cm/s and the average Al/B atomic concentration between 1×10^{17}cm^{-3} and 2×10^{19}cm^{-3}. From the Fig.9, it can be seen that the oxygen trap level obviously impacts the electronic properties only when the BSRV is either less than 1×10^{5}cm/s or the average Al/B atomic concentration is less than 1×10^{18}cm^{-3}. Especially, when the average Al/B atomic concentration is around 1×10^{17}cm^{-3}and the BSRV is 3×10^{2}cm/s, the oxygen trap level greatly impacts the photoelectric conversion efficiency with a disparity of around 1%. In other words, the other trap levels of above impurities in Al-BSF have a less impact on the electronic properties of solar cells in this case of the BSRV less than 1×10^{5}cm/s or the average Al/B atomic concentration less than 1×10^{18}cm^{-3}. Conclusively, the trap levels of impurities in Al-BSF have a slight effect on the electronic properties of solar cells, especially in this case of the BSRV more than 1×10^{5}cm/s or the average Al/B atomic concentration more than 1×10^{18}cm^{-3}.

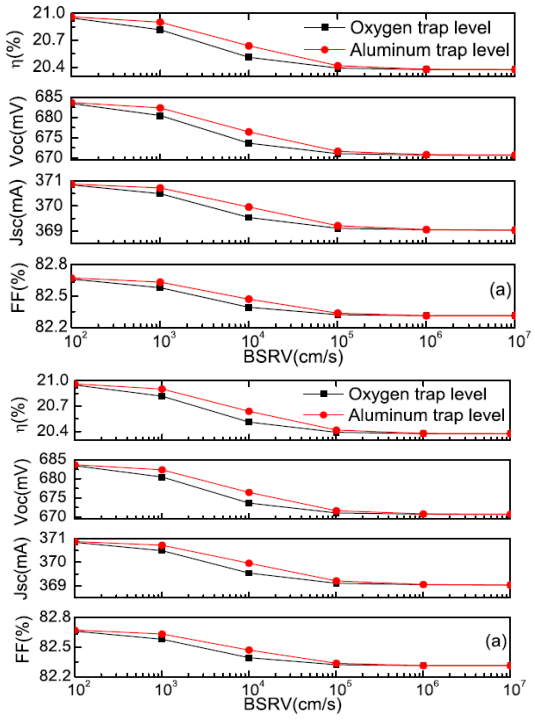

Fig.9 The effect of the oxygen trap level on the electronic properties of solar cells:(a) with the average Al/B atomic concentration of 5×10^{18}cm^{-3}; (b) with the BSRV of 1×10^{3}cm/s

4 Conclusions

We have analyzed the effect of the Al-BSF on electronic properties of n^+pp^+ monocrystalline solar cells. The electronic properties of solar cells are completely independent of the gradient of the doping profile of the Al-BSF, but mainly depend on the Al/B atomic amount in the Al-BSF when the average Al/B atomic concentration in Al-BSF is not more than around $6.56\times10^{18}cm^{-3}$. Besides, the electrical properties decline gradually with the increase of Al/B-BSF thickness when the average Al/B atomic concentration in Al-BSF is about between ~$6.56\times10^{18}cm^{-3}$ and ~$1.15\times10^{19}cm^{-3}$. The electronic properties of the solar cells are optimized if the average Al/B atomic concentration and thickness of Al/B-BSF are about $6.56\times10^{18}cm^{-3}$ and 10μm respectively. The optimum thickness of BSF declines sharply with the average Al/B atomic concentration of Al-BSF more than ~$1.15\times10^{19}cm^{-3}$ mainly depends on the diffusion length of minority carriers in heavily-doped BSF region. The trap levels of impurities in Al-BSF have a slight effect on the electronic properties of solar cells. Especially, in this case of the BSRV more than ~1×10^5cm/s or the average Al/B atomic concentration more than ~$1\times10^{18}cm^{-3}$, these effects of the trap levels are even almost negligible.

Acknowledgements

This work was financially supported by the Hunan Province Grand Science and Technology Special Project under the contract No. 08FJ1002. Thanks are also owned to the ARC Photovoltaics Centre of Excellence in University of New South Wales for providing the free program PC1D.

References

[1] J. H. Zhao, A. H.Wang, M. A Green, Solar Energy Materials &Solar Cells **66**, 27 (2001)
[2] Y. Tsunomura, Y. Yoshimine, M. Taguchi, T. Kinoshita, H. Kanno, H. Sakata, E. Maruyama, M. Tanaka, Solar Energy Materials &Solar Cells **93**, 670 (2007)
[3] J. Benick, B. Hoex, M. C. M. van de Sanden, W. M. M. Kessels, O.Schultz, S.W. Glunz, Applied Physics Letters **92**, 3504 (2008)
[4] S. Narasimha, A. Rohatgi, A. W. Weeber, IEEE Transactions On Electron Devices **46**, 1363 (1999)
[5] V. Meemongkolkiat, K. Nakayashiki, D. S. Kim, R. Kopecek, A. Rohatgi, Journal of The Electrochemical Society **153**(1), G53 (2006)
[6] P. S. Plekhanov, M. D. Negoita, T. Y. Tan, Journal of Applied Physics **90**, 5388 (2001)
[7] D. Abdelbarey, V. Kveder, W. Schröter, M. Seibt, Applied Physics Letters 94, 1912 (2009)
[8] D. H. Neuhaus, A. Münzer, Advanced Optoelectronics 2007, 24521(2007)
[9] A. G. Aberle, Progress in Photovoltaics: Research and Applications **8**, 473 (2000)
[10] J. Schmidt, M. Kerr, A. Cuevas, Semiconductor Science and technology**16**, 164(2001)
[11] R. Bock, J. Schmidt, R. Brendel, Applied Physics Letters **91**, 2112 (2007)
[12] J. M. Kim, Y. K. Kim, T. Pham, Solar Energy Materials &Solar Cells **86**, 577 (2005)
[13] P. Lölgen, W. C. Sinke, C. Leguijt, A. W. Weeber, P. F. A. Alkemade, L. A.Verhoef, Applied Physics Letters **65**, 2792 (1994)
[14] P. A. Kaminski, B. Vandelle, A. Fave, J. P. Boyeaux, L. Q. Nam, R. Monna, D. Sarti, A. Laugier, Sol. Solar Energy Materials &Solar Cells **72**, 373 (2002)
[15] R. Lago-Aurrekoetxea, C. del Cañizo, I. Tobías, A. Luque, Solid-State Electronics **49**, 49 (2005)
[16] N. Stem, C. A. S. Ramos, M. Cid, Solid-State Electronics **54**, 221 (2010)
[17] P. Kittidachachan, T. Markvart, D. M. Bagnall, R. Greef, G. J. Ensell, Solar Energy Materials &Solar Cells **91**, 160 (2007)
[18] P. A. Basore, D. A. Clugston, User Manual for PC1D (Version 5.9), University New South Wales, Sydney, Australia, 2003
[19] J. A. Amick, F. J. Bottari, J. I. Hanoka, Journal of The Electrochemical Society **141**, 1577 (1994)
[20] J. G. Fossun, IEEE Transactions On Electron Devices **24**, 322 (1977)
[21] M. J. Kerr, Surface, Emitter and Bulk Recombination in Silicon and Development of Silicon Nitride Passivated Solar Cells, A thesis for the degree of Doctor of Philosophy of the Australian National University, Canberra, Australia, 2002
[22] J.Tan, A. Cuevas, D. Macdonald, D. Bätzner, H. Mäckel, K. Hanto, Measurement and optimization of the recombination current of p^+ aluminum doped regions. In Proceeding of the 21th Photovoltaic Solar Energy Conference and Exhibition, WIP-Renewable Energies, Munich, Germany, 2006
[23] A. Cuevas, R. A. Sinton, Detailed modelling of silicon solar cells. In Proceeding of the 23rd Photovoltaic Solar Energy Conference and Exhibition, WIP-Renewable Energies, Munich, Germany, 2008
[24 M. A. Green, IEEE Transactions On Electron Devices **31**, 671 (1984)
[25] A. K. Liu, B. S. Zhu, J. S. Luo, Semiconductor physics (the Seventh edition), Publishing house of electronics industry, Beijing, 2008
[26] G. A. M. Hurkx, D. B. M. Klaassen, M. P. G. Knuvers, IEEE Transactions On Electron Devices **39**, 331 (1992)

*Corresponding author: chenyongmin@foxmail.com